engineering proceedings

MDPI

Proceeding Paper

Study of the Negative Work Area in the p-V Diagram of an HCCI Engine †

Csaba Tóth-Nagy

Department of Propulsion Technology, Audi Hungaria Faculty of Vehicle Engineering, Széchenyi István University, Egyetem tér 1, H 9026 Győr, Hungary; toth-nagy.csaba@ga.sze.hu; Tel.: +36-30-277-4030

† Presented at the Sustainable Mobility and Transportation Symposium 2024, Győr, Hungary, 14–16 October 2024.

Abstract: Homogeneously charged compression ignition is a promising combustion process that is proven to increase combustion efficiency and decrease exhaust emissions when compared to Otto or Diesel engine efficiencies and emissions. The HCCI process can be considered an advancement on the path to sustainability. However, improper control of the start of combustion causes the efficiency of the engine to drop significantly. The reason for this efficiency drop is that an early start of combustion causes the piston on the upward stroke to experience increased cylinder pressure after the combustion process is complete. The piston must further compress the cylinder content until it reaches the top dead center. During this process, the piston still experiences an increased gas force on the way towards TDC, having to invest extra disadvantageous work into the compression stroke, causing a negative work area in the pressure–volume diagram of the engine. The present study introduces the negative work area in the p-V diagram of an HCCI engine. It describes the phenomenon and explores the reasons behind it. It also investigates some of the factors affecting the negative work area in the p-V diagram.

Keywords: negative work; HCCI; knocking; combustion; internal combustion engine

check for updates

Citation: Tóth-Nagy, C. Study of the Negative Work Area in the p-V Diagram of an HCCI Engine. *Eng. Proc.* **2024**, *79*, 22. https://doi.org/10.3390/engproc2024079022

Academic Editors: András Lajos Nagy, Boglárka Eisinger Balassa, László Lendvai and Szabolcs Kocsis-Szürke

Published: 4 November 2024

Copyright: © 2024 by the author. Licensee MDPI, Basel, Switzerland. This article is an open access article distributed under the terms and conditions of the Creative Commons Attribution (CC BY) license (https://creativecommons.org/licenses/by/4.0/).

1. Introduction

Over the past 20 years, the propulsion of passenger cars has undergone significant transformation. The advancement of power electronics has brought about developments in electric drives; however, the current shortcomings of batteries only allow for purely electric propulsion within certain limitations. Nevertheless, to reduce emissions and consumption, hybrid electric drivetrains are becoming increasingly popular in today's vehicles, serving as an intermediate step in the electrification process. In 2023, one in four cars sold in the European Union was a hybrid electric vehicle [1].

Among the architectures used in hybrid drivetrains is the series hybrid [2]. In a series hybrid, an auxiliary power unit generates electrical energy, which can either drive the wheels through an electric motor, charge the battery for later use, or do both simultaneously. In the field of auxiliary power units, alongside the traditional internal combustion engine-driven rotary generator, there is the free-piston internal combustion engine-driven linear generator [3]. The unique feature of the free-piston internal combustion engine is that it lacks a crankshaft, with all moving parts performing linear reciprocating motion. One possible way to extract energy from a free-piston engine is through an attached linear generator, converting the energy into an electrical form. Thus, the free-piston engine coupled with a linear generator unit could be a suitable candidate for the auxiliary power unit in hybrid electric vehicles [4].

Besides driving a linear generator [5], free-piston engines are proposed to be applied coupled with hydraulic pumps [6] and pneumatic pumps [7].

This paper studies a phenomenon observed in an HCCI (homogeneously charged compression ignition) free-piston engine: the negative work area around top dead center

observed with excessive fuel input relative to the given load. The aim is to gain insight into the influence on the negative work area in the p-v diagram. It is important to note that HCCI operation itself does not cause the appearance of the negative work area, as the optimal start of combustion should happen exactly at TDC. Besides rapid burning, the advancement of autoignition is necessary to cause the negative work area to appear.

2. Methods

2.1. The HCCI Free-Piston Engine Prototype

Tóth-Nagy [4] introduces a free-piston internal combustion engine and reports on the phenomenon of the negative work area without exploring or explaining it. The theoretical layout of the two-cylinder free-piston internal combustion engine is shown in Figure 1.

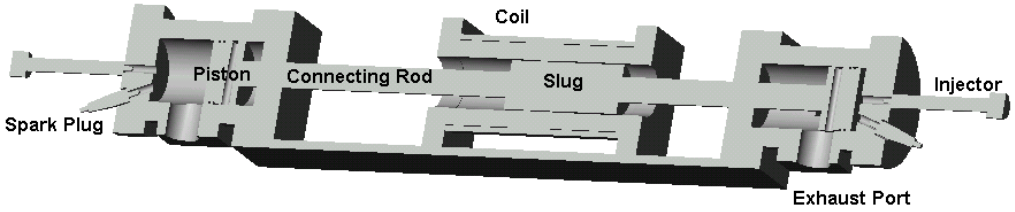


Figure 1. Theoretical layout diagram of the HCCI free-piston internal combustion engine prototype.

Where possible, the engine components were sourced from commercially available parts, such as two-stroke cylinders, cylinder heads, spark plugs, pistons, piston rings, and wrist pins, as well as elements of a common rail diesel injection system. Intake air was supplied from an external source as it is a prototype engine. Fuel injection was controlled by a microcontroller and driver circuit developed during this research. The static parameters included a bore of 76 mm, an effective stroke of 38 mm, a total possible stroke of 73.8 mm, a fuel mass of 0.003108 g per injection, a maximum load force of 138 N, and an injection timing of 10 mm before the TDC. The measured dynamic parameters were an operating frequency of 53 Hz, a mechanical efficiency of 11%, and an output power of 1080 W. As the engine used two-stroke cylinders, lubrication was provided through mixing lubricant into the fuel. Spark plugs were only needed during engine start-up. Toth-Nagy et al. have also experimented with the design variables in order to optimize engine performance [8].

The measuring and data acquisition system was developed for the engine during this research. The measured quantities included the cylinder pressure in both cylinders and the position of the reciprocating mass. Pressure was measured using PCB piezo-crystal sensors, and translator position was measured using a Micro-Epsilon inductivity-type non-contact position sensor. Measured data were synchronized in an off-line fashion during data processing after the measurements were carried out. Using these data, a p-V diagram was created to study the phenomena occurring in the engine cylinders. The p-V diagram is shown in Figure 2. The loop describing the behavior around top dead center was conspicuous. At first glance, the phenomenon seemed to be a measurement error, which could be corrected by synchronizing the pressure and position data over time, which was carried out. The synchronized data of cylinder pressure and position are shown in Figure 3. The synchronization of cylinder pressure and position data was carried out on a dataset where there was no combustion during a shutdown. Such a shutdown event is shown in Figure 4.

Figures 2 and 3 show data where cylinder pressure and position data are already synchronized over time.

The negative work area is visible in Figure 2. The negative work area appears when a relatively fast heat release happens and all the (or a vast majority of the) fuel mass burns before TDC. After further compressing the cylinder content, the piston passes TDC. A negative work area is observable at around ignition TDC when cylinder pressure is lower on the expansion stroke than that on the preceeding compression stroke. The arrows in Figure 2 indicate the evolution of pressure vs. translator position.

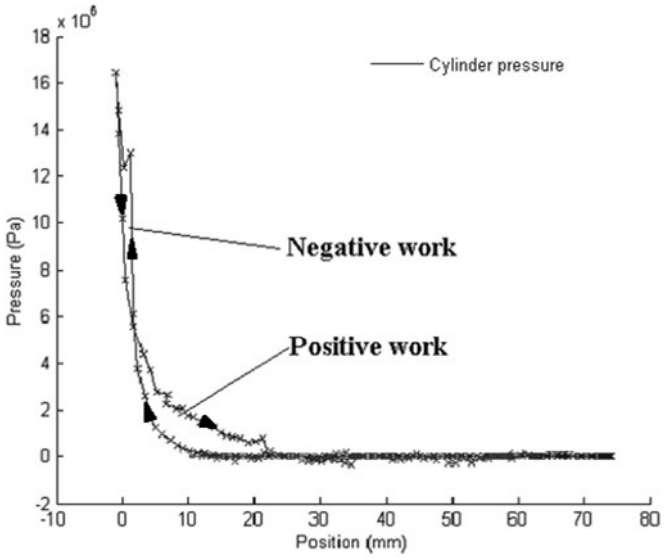


Figure 2. p-V curve of the free-piston engine, showcasing the evolution of cylinder pressure under firing at 10% throttle and no load.

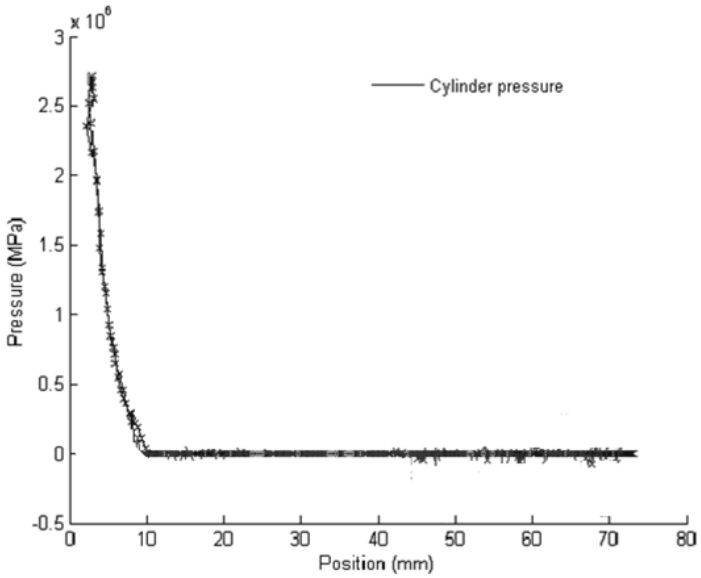


Figure 3. p-V curve of the free-piston engine, showcasing the evolution of cylinder pressure under motored conditions.

2.2. Simulation Model

A time-based simulation model was developed in Matlab R12 to investigate this phenomenon using dynamic differential equations of motion. Figure 4 shows the free-body diagram that forms the basis of the model. The dynamic model calculates the acceleration of the reciprocating mass, and then from the acceleration, it calculates the velocity and position using numerical integration.

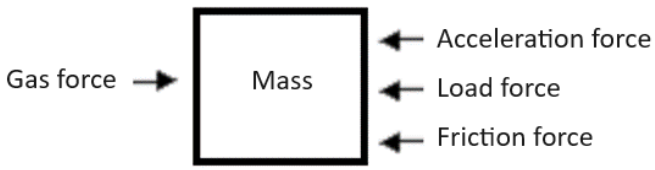


Figure 4. Free-body diagram of the reciprocating mass of the free-piston engine. Acceleration force = Gas force-Load force-Friction force.

Gas force was calculated from the cylinder pressure, which was determined by the first law of thermodynamics (Equation (1)). The temperature of the cylinder was calculated by the ideal gas law (Equation (2)). The model uses a double Wiebe function-based [9] heat release equation proposed by Shoukry [10] (Equation (3)). Modification was made to the equation to approach the behavior of HCCI, i.e., close to instantaneous heat release, by varying Mp (premixed bun coefficient) and Md (diffusion burn coefficient). The model also accounts for thermodynamic heat losses (temperature-dependent model) and blow-by past the piston rings (pressure-dependent model) in calculating the gas force, enabling the appearance of the negative work area loop on the p-V diagram.

$$\frac{dp}{dt} = -\gamma \frac{p}{V}\frac{dV}{dt} + (\gamma - 1)\frac{1}{V}\frac{dQ}{dt} \quad (1)$$

$$T = \frac{pV}{mR_{air}} \quad (2)$$

$$\frac{dQ}{dt} = a\frac{Q_p}{t_p}(M_p + 1)(\frac{t}{t_p})^{M_p} exp(-a(\frac{t}{t_p})^{M_p+1}) + a\frac{Q_d}{t_d}(M_d + 1)(\frac{t}{t_d})^{M_d} exp(-a(\frac{t}{t_d})^{M_d+1}) \quad (3)$$

$$Fg = Blv \quad (4)$$

$$F_l = F_n v \quad (5)$$

Load (F_l) (Equation (5)) was modeled as friction on the translator using a varying normal force (F_n) and constant friction coefficient (μ) multiplied by translator speed (v) in addition and similarly to modeling the internal friction of the engine. This was considered acceptable because, on the one hand, a generator (Equation (4)) behaves somewhat similarly to a frictional load (Equation (5)) as both are a function of translator velocity. The varying friction coefficient represents the varying load of the linear generator coupled to the linear engine. On the other hand, the prototype engine was also loaded through a friction brake. Hence, it was a logical method to also replace the generator with a friction load in the model, simplifying the validation process.

2.3. Validation

The simulation model was validated based on measurements carried out on the free-piston engine prototype. Figure 5 compares the position of the reciprocating mass of the engine during shutdown with simulated and measured values.

Figure 6 shows the measured vs. simulated translator position. Based on the validations, the simulation model proved suitable for studying the negative work area appearing on the p-V diagram.

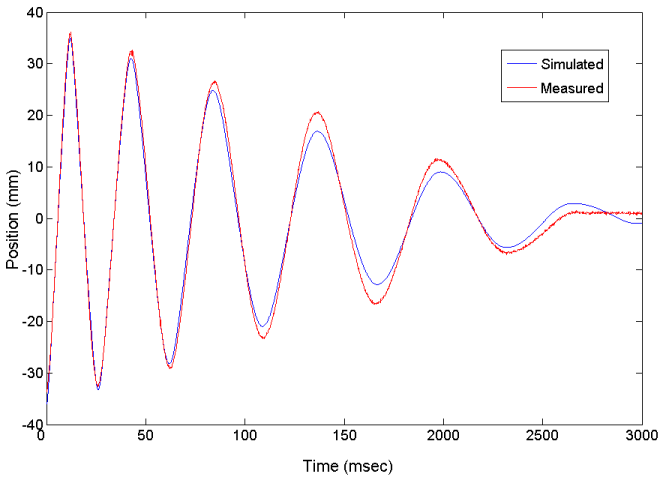


Figure 5. Position of the reciprocating mass of the engine during shutdown.

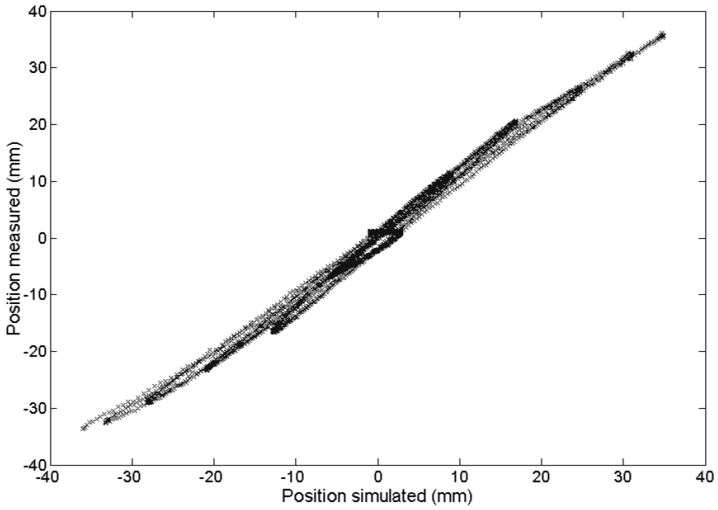


Figure 6. Simulated vs. experimental translator position after engine was turned off (ringing down). Correlation coefficient: 0.995.

3. Results and Discussions

The simulation results are shown in Figure 7. The p-V diagram drawn from the simulation results also shows the negative work area observed around top dead center. Figure 8 zooms in on the critical part of the curve, clearly showing the negative work area. The increase in the negative work area and the shift of top dead center result from the decreasing load. Increasing blow-by and heat transfer to the cylinder wall, as well as increasing the fuel injection rate, are believed to have a similar effect, as does increasing the heat release rate. Simulation was carried out at 5% throttle, and the load was varied from the maximum permissible load at the given throttle (curve 1) through many intermediate load scenarios, of which only one is indicated (curve 2) to include no load at all (curve 3). This clearly shows the development of the negative work area.

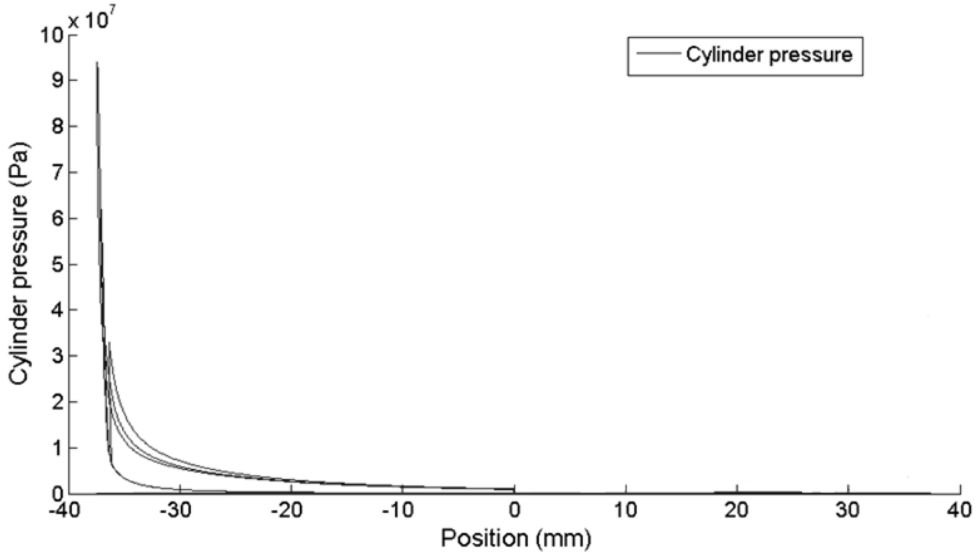


Figure 7. Simulation result: p-V diagram, cylinder pressure vs. piston position.

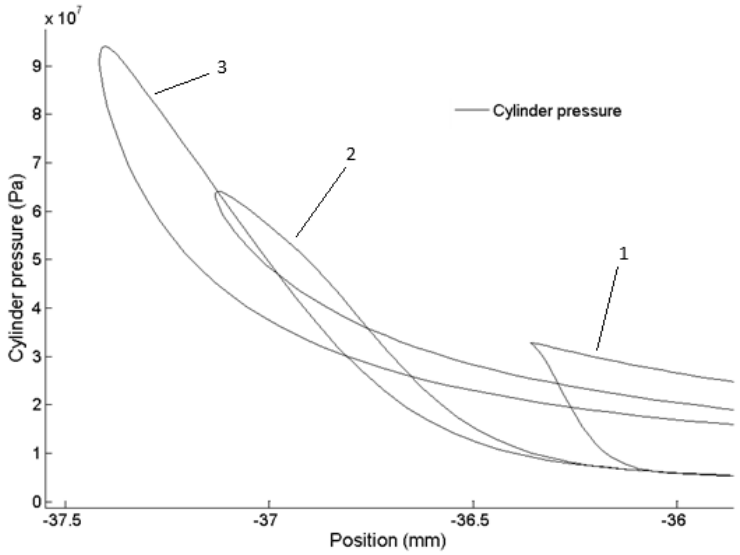


Figure 8. Simulation result: p-V diagram, cylinder pressure vs. piston position. Cylinder pressure–position with negative work area zoomed in on. Data are the same as presented in Figure 7.

The negative work area became apparent due to three factors: two-stroke cylinders were used, it is a free-piston engine without a predefined TDC, and the engine operated in an HCCI combustion fashion. First, the two-stroke engine has greater blow-by between the cylinder wall and piston rings, which increases the negative work area, facilitating its formation and observation. Second, since the engine is a free-piston engine, the piston does not reverse at a determined top dead center due to the constraining effect of a slider–crank mechanism, as there is no slider–crank mechanism and no constraining effect. Instead, it approaches the cylinder head more closely, further compressing the charge. The only constraining effect in the cylinder is the increasing pressure due to compression, acting like an air spring returning the piston. Third, the HCCI mode significantly contributed to the amplification of the phenomenon, allowing its observation. In slower traditional combustion, the fuel does not have time to burn before reaching the top dead center, as it extends over a longer time, and most of the heat release and pressure increase occur after the top dead center, increasing the positive work area. During HCCI operation, combustion happens quasi-instantaneously in an extremely short time and with an extremely high heat release rate, causing most of the fuel to burn before the top dead center, resulting in the loop observed at the TDC described as the negative work area. The negative work area grows as the uncontrolled start of combustion advances. However, proper control of the start of combustion (right at the TDC) will eliminate the negative work area and improve the efficiency of a free-piston engine.

4. Conclusions

The experiments with the prototype engine have proven that the negative work area observed on the p-V diagram was not an error. The simulation model virtually reproduced the phenomenon, proving that the negative work area is real. The simulation model showed that the negative work area increases as load decreases or as the start of combustion advances. It can also be concluded that proper control of the start of combustion (optimally at the TDC) will eliminate the negative work phenomenon, optimizing the efficiency of the engine.

Future work will have to investigate the effect of varying blow-by, heat transfer to the cylinder wall, the fuel injection rate, and the heat release rate.

Funding: This research received no external funding.

Institutional Review Board Statement: Not applicable.

Informed Consent Statement: Not applicable.

Data Availability Statement: Data for this study are available upon request from the corresponding author.

Conflicts of Interest: The author declares no conflicts of interest.

Nomenclature

a	Constant
cp	Specific heat at constant pressure
cv	Specific heat at constant volume
Fl	Load force
γ	Ratio of specific heats (cp/cv)
μ	Friction coefficient
Md	Diffusion burn coefficient
Mp	Premix burn coefficient
p	Cylinder pressure
$\frac{dQ}{dt}$	Heat release rate
Qd	Heat released in the diffusion burn
Qp	Heat released in the premix burn
Re	Reynold's number
t	Actual time
T	Average charge temperature
td	Time that the diffusion burn takes
tp	Time that the premix burn takes
V	Volume

References

1. European Automobile Manufacturers' Association (ACEA). New Car Registrations: +13.9% in 2023; Battery Electric 14.6% Market Share. ACEA. 2024. Available online: https://www.acea.auto/pc-registrations/new-car-registrations-13-9-in-2023-battery-electric-14-6-market-share (accessed on 3 October 2024).
2. Conley, J.; Taylor, S.; Atkinson, C.; Tóth-Nagy, C.; Smith, J.; Waters, R.; Clay, B. Development of a Fourth Generation Hybrid Electric Vehicle at West Virginia University. In Proceedings of the SAE 2001 World Congress, Detroit, MI, USA, 5–8 March 2001. SAE Technical Paper 2001-01-0682. [CrossRef]
3. Tóth-Nagy, C.; Clark, N. The linear engine in 2004. In Proceedings of the 2005 SAE Brasil Fuels & Lubricants Meeting, Rio de Janeiro, Brazil, 11–13 May 2005. SAE Technical Paper 2005-01-2140. [CrossRef]
4. Tóth-Nagy, C. Application of Linear Engines in Series Hybrid Vehicles. Ph.D. Thesis, West Virginia University, Morgantown, WV, USA, 2004.
5. Guo, C.; Wang, Y.; Tong, L.; Feng, H.; Zuo, Z.; Jia, B. Research on Piston Dynamics and Engine Performances of a Free-Piston Engine Linear Generator Coupling with Various Rebound Devices. *Energies* **2023**, *16*, 6570. [CrossRef]
6. Ma, F.; Zhang, S.; Zhao, Z.; Wang, Y. Research on the Operating Characteristics of Hydraulic Free-Piston Engines: A Systematic Review and Meta-Analysis. *Energies* **2021**, *14*, 3530. [CrossRef]
7. Underwood, A.F. *The GMR 4-4 "HYPEREX" Engine. A Concept of the Free-Piston Engine for Automotive Use*; SAE Technical Paper 570032; SAE: Warrendale, PA, USA, 1957.
8. Toth-Nagy, C.; Farmouri, P.; Clark, N. Compression Ignition Linear Engine Design Variable Effects. In Proceedings of the Internal Combustion Engine Division Fall Technical Conference, Vancouver, BC, Canada, 23–26 September 2012; ICEF2011-60157. pp. 1029–1036.
9. Wiebe, I.I.; Farafanov, M.F. Analysis of engine cycles using digital computers. *Tract. Agric. Mach.* **1967**, *6*, 232–250. (In Russian)
10. Shoukry, E.F. Numerical Simulation for Parametric Study of a Two-Stroke Compression Ignition Direct Injection Linear Engine. Ph.D. Thesis, West Virginia University, Mechanical and Aerospace Engineering Department, Morgantown, WV, USA, 2003.

Disclaimer/Publisher's Note: The statements, opinions and data contained in all publications are solely those of the individual author(s) and contributor(s) and not of MDPI and/or the editor(s). MDPI and/or the editor(s) disclaim responsibility for any injury to people or property resulting from any ideas, methods, instructions or products referred to in the content.